Neurobiology of Disease

Corticospinal Motor Neurons and Related Subcerebral Projection Neurons Undergo Early and Specific Neurodegeneration in hSOD1^{G93A} Transgenic ALS Mice

P. Hande Özdinler,[1,2,3] Susanna Benn,[4] Ted H. Yamamoto,[1,2,3] Mine Güzel,[1,2,3] Robert H. Brown Jr,[4] and Jeffrey D. Macklis[1,2,3]

[1]MGH-HMS Center for Nervous System Repair, Departments of Neurosurgery and Neurology, and Program in Neuroscience, Harvard Medical School, [2]Nayef Al-Rodhan Laboratories, Massachusetts General Hospital, and [3]Department of Stem Cell and Regenerative Biology and Harvard Stem Cell Institute, Harvard University, Boston, Massachusetts 02114, and [4]Department of Neurology, MassGeneral Institute for Neurodegenerative Diseases, Massachusetts General Hospital, Harvard Medical School, Charlestown, Massachusetts 02129

Amyotrophic lateral sclerosis (ALS) is characterized by predominant vulnerability and central degeneration of both corticospinal/corticobulbar motor neurons (CSMN; "upper motor neurons") in cerebral cortex, and spinal/bulbar motor neurons (SMN; "lower motor neurons") in spinal cord and brainstem. Increasing evidence indicates broader cerebral cortex pathology in cognitive, sensory, and association systems in select cases. It remains unclear whether widely accepted transgenic ALS models, in particular hSOD1^{G93A} mice, undergo degeneration of CSMN and molecularly/developmentally closely related populations of nonmotor projection neurons [e.g., other subcerebral projection neurons (SCPN)], and whether potential CSMN/SCPN degeneration is specific and early. This relative lack of knowledge regarding upper motor neuron pathology in these ALS model mice has hindered both molecular-pathophysiologic understanding of ALS and their use toward potential CSMN therapeutic approaches. Here, using a combination of anatomic, cellular, transgenic labeling, and newly available neuronal subtype-specific molecular analyses, we identify that CSMN and related nonmotor SCPN specifically and progressively degenerate in hSOD1^{G93A} mice. Degeneration starts quite early and presymptomatically, by postnatal day 30. Other neocortical layers, cortical interneurons, and other projection neuron populations, even within layer V, are not similarly affected. Nonneuronal pathology in neocortex (activated astroglia and microglia) is consistent with findings in human ALS cortex and in affected mouse and human spinal cord. These results indicate previously unknown neuron type-specific vulnerability of CSMN/sensory and association SCPN, and identify that characteristic dual CSMN and SMN degeneration is conserved in hSOD1^{G93A} mice. These results provide a foundation for detailed investigation of CSMN/SCPN vulnerability and toward potential CSMN therapeutics in ALS.

Introduction

Independent, but presumed to be mechanistically related, degeneration of both "upper" [corticospinal/corticobulbar motor neurons (CSMN)] and "lower" [spinal/bulbar motor neurons (SMN)] components of motor neuron circuitry (Lefebvre et al., 1998; Gavrilina et al., 2008) distinguishes amyotrophic lateral sclerosis (ALS) from disorders characterized by marked vulnerability and degeneration of either SMN in spinal muscular atrophy (SMA) (Rösler et al., 2000; Beckman et al., 2001; Brown and Robberecht, 2001; Bruijn et al., 2004; Stewart et al., 2006; Turner and Talbot, 2008) or CSMN in hereditary spastic paraplegia (HSP) and sporadic primary lateral sclerosis (PLS) (Fink, 2002, 2006; Rainier et al., 2003). ALS is a "system degeneration disorder," with progressive degeneration of both CSMN and SMN, with increasing evidence for involvement of broader cortical neuronal and widely distributed nonneuronal pathology (Lomen-Hoerth et al., 2003; Strong, 2008), including astrogliosis and activated microglia in the neocortex of select ALS patients (Graham et al., 2004; Brown, 2005; Stewart et al., 2006).

Both inherited (familial) and sporadic forms of ALS show similar cardinal features: clinical course and neuropathology (Bendotti and Carrì, 2004; Boillée and Cleveland, 2004; Bruijn et al., 2004; Pasinelli and Brown, 2006). Thus, transgenic mouse models generated based on genetics of even relatively rare inherited forms of ALS offer important tools with which to investigate both sporadic and familial ALS, if patient pathology is faithfully reflected (Gurney, 1997, 2000). Toxic "gain of function" mutation in the *superoxide dismutase-1* (*SOD1*) gene, linked to ~10–

Received Aug. 10, 2010; revised Dec. 20, 2010; accepted Jan. 24, 2011.

This work was supported by grants from the National Institutes of Health (NS49553; additional infrastructure provided by NS41590 and NS45523), the ALS Association, and the Harvard Stem Cell Institute to J.D.M., and the Les Turner ALS Foundation to P.H.O. P.H.O. was partially supported by a fellowship from the Harvard NeuroDiscovery Center, and by a program grant from the Harvard Stem Cell Institute to J.D.M. We thank K. Billmers, A. Palmer, A. Sanders, M. Jonathan for technical assistance; members of the Macklis and Brown laboratories for important input and suggestions; and E. Azim, S. Sohur, and J. Emsley for critical reading of an earlier version of this manuscript.

P. H. Özdinler's present address: Department of Neurology, Northwestern University, Feinberg School of Medicine, Chicago IL 60611.

R. H. Brown Jr's present address: Department of Neurology, University of Massachusetts Medical School, Worcester, MA 01655.

Correspondence should be addressed to Jeffrey D. Macklis at the above address, E-mail: jeffrey_macklis@hms.harvard.edu; or P. Hande Özdinler at her present address, E-mail: ozdinler@northwestern.edu.

DOI:10.1523/JNEUROSCI.4184-10.2011

 0270-6474/11/314166-12$15.00/0

20% of familial ALS (~1–2–5% of all cases) is known to result in an ALS-like SMN degeneration phenotype in hSOD1^{G93A} transgenic mice (Gurney et al., 1994; Tu et al., 1996; Gurney, 1997; Kunst et al., 1997; Beckman et al., 2001; Wong et al., 2002; Bendotti and Carrì, 2004; Wengenack et al., 2004; Hegedus et al., 2007). In contrast to considerable investigation of SMN in hSOD1^{G93A} and other models (Chiu et al., 1995), much less is known about cortical components [degeneration of CSMN and subcerebral projection neurons (SCPN) that constitute cognitive, association, and integrative sensory circuitry (Zang and Cheema, 2002; Lobsiger et al., 2005; Yamanaka et al., 2006), and whether widely distributed nonneuronal pathology observed in select ALS patients is recapitulated in hSOD1^{G93A} mice].

Reports on hSOD1^{G93A} mice have suggested that their neuropathology is restricted mainly to spinal and bulbar motor neuron degeneration, but not in cortex (Wong et al., 2002; Ralph et al., 2005; Niessen et al., 2006), potentially suggesting that hSOD1^{G93A} mice do not represent the complete human ALS phenotype. The lack of data on CSMN is perhaps not surprising, since only ~6000 CSMN exist per hemisphere in mice, intermixed with millions of other cortical pyramidal neurons in the same region and layer V of motor cortex. Identification of specific degeneration of CSMN and related SCPN is enabled with recently identified molecular markers and knowledge about CSMN/SCPN developmental relationship (Gurney, 2000; Arlotta et al., 2005; Molyneaux et al., 2005, 2007, 2009; Tomassy et al., 2010). A few studies report corticospinal tract involvement in hSOD1^{G93A} mice (Zang and Cheema, 2002; Lobsiger et al., 2005; Yamanaka et al., 2006), although complexities noted above limited analyses. One study, using retrograde labeling from spinal cord at postnatal day 60 (P60), reported CSMN loss (Zang and Cheema, 2002), although it was difficult to assess the following: (1) whether observed reduction in retrogradely labeled neurons was due to abnormal retrograde axonal transport or true neuronal loss; (2) whether specific CSMN degeneration or broader cortical degeneration occurs; (3) whether observed abnormalities develop before P60; or (4) whether broader populations of SCPN/other neurons are affected.

To provide a foundation for increasingly detailed investigation of CSMN/SCPN biology in ALS and for critical analysis of cellular and molecular mechanisms of shared biology between CSMN/SCPN and SMN components of motor neuron circuitry, we investigated whether distinct and specific degeneration of CSMN (with additional but not yet clarified non-CSMN cortical degeneration), as observed in ALS patients (Rösler et al., 2000; Zanette et al., 2002; Stewart et al., 2006), is faithfully reproduced in hSOD1^{G93A} mice. Our results allow increasingly detailed cellular and molecular investigation of the biology of CSMN and broader molecularly and developmentally related populations of SCPN in hSOD1^{G93A} mice. Elucidating this CSMN/SCPN biology might potentially contribute toward development of preventive and/or reparative therapeutics for ALS and related CSMN/SCPN degenerative diseases.

Materials and Methods

Mice. Male and female wild-type (WT), hemizygous transgenic mice overexpressing the wild-type human SOD1 gene (hSOD1^{WT}), and hemizygous transgenic mice expressing the SOD1 gene containing the G93A mutation in (hSOD1^{G93A}) were used (Fig. 1*A*). All mouse strains are on the C57BL/6 background, and the range of gene copy number, determined before surgery, was the same in hSOD1^{G93A} and hSOD1^{WT} mice (30 ± 2). Thy1-YFP-hSOD1^{G93A} and Thy1-YFP-hSOD1^{WT} mice were generated by breeding Thy1-YFP mice [gift from J. Sanes, Harvard University, Boston, MA (Bareyre et al., 2005)] and hemizygous hSOD1^{G93A} or hSOD1^{WT} transgenic mice, respectively. Thy1-YFP;WT mice were used as controls. All mouse studies were approved by the Massachusetts General Hospital Institutional Animal Care and Use Committee and performed in accordance with institutional, federal, and National Institutes of Health guidelines.

CSMN labeling and tissue collection. CSMN were retrogradely labeled via stereotactic FluoroGold injections (2% FG, 250 nl/mouse) into the cervical region (C4–C6) of the corticospinal tract within the dorsal funiculus of the spinal cord at distinct, phenotypically distinguishable times defined previously (Gurney et al., 1994; Tu et al., 1996; Hall et al., 1998; Cleveland and Rothstein, 2001; Wengenack et al., 2004; Hegedus et al., 2007) as P20, "early"; P50, "symptomatic"; and P110, "end stage." In a subset of experiments, mice injected at P50 were perfused at P120 to distinguish between genuine CSMN degeneration and potential appearance of reduced FG labeling due to defects in axonal transport (Fig. 1*A*, "#"). Ten days after FluoroGold injection, mice were deeply anesthetized and perfused with cold 0.1 M PBS supplemented with heparin, followed by cold 4% paraformaldehyde (PFA) in 0.1 M PBS. To further investigate whether degeneration of other neocortical projection neurons with equivalently long axons [most notably, interhemispheric callosal projection neurons (CPN)] occurs, in a subset of experiments dual CPN and CSMN retrograde labeling was performed in hSOD1^{G93A} and WT mice at P30, and mice were perfused at P120. CPN were retrogradely labeled via stereotactic injection of green fluorescent microspheres into contralateral cortex (250 nl/mouse), and CSMN were retrogradely labeled via stereotactic injection of red fluorescent microspheres (250 nl/mouse) into the cervical region (C4–C6) of the corticospinal tract within the dorsal funiculus of the spinal cord. Brains were postfixed in 4% PFA overnight, and 40 μm thick coronal sections were cut on a Leica VT 1000S vibrating microtome.

Immunocytochemistry, Nissl staining, and in situ *hybridization.* All immunocytochemical procedures were performed on every twelfth tissue section of 40-μm-thick coronal sections. The following primary antibodies were used: FG (1:500, Millipore Bioscience Research Reagents), CTIP2 (1:200, Calbiochem), LMO4 (1:200, Santa Cruz Biotechnology), cleaved caspase 3 (1:250, Cell Signaling), parvalbumin (PV; 1:500, Sigma), neuropeptide Y (NPY; 1:500, Immunostar), GFAP (1:200, Santa Cruz Biotechnology), CD68 (1:100, Millipore Bioscience Research Reagents), and FoxP2 (1:250, Abcam). Appropriate secondary fluorescent antibodies (1:500, Alexa 488 and 546, Invitrogen) were applied in blocking solution at room temperature, in the dark, for 2–4 h. CTIP2 and LMO4 immunocytochemical analysis were enhanced by increased primary antibody incubation (2 d) at 4°C, and 1:200 dilution was used for secondary fluorescent antibodies at 4°C overnight. Nuclear counterstain (ToPro; 1:5000 in 0.1 M PBS) was used to investigate nuclear pyknosis. Nissl staining was performed on every twelfth comparable section (40 μm thick, coronal) isolated from WT, hSOD1^{WT}, and hSOD1^{G93A} mice. *Cry-mu*, *Igfbp4*, *Cux2*, *Fezf2*, and *PlexinD1* probes were prepared, and *in situ* hybridization analysis was performed as previously described (Molyneaux et al., 2005, 2009).

Imaging, quantification, and statistical analysis. Sections were mounted on slides and analyzed using a Nikon E1000 fluorescence microscope equipped with an X-Cite 120 illuminator (EXF0), and images were acquired using a cooled charge-coupled device digital camera (Q Imaging Retiga EX). Confocal images were collected using a Bio-Rad Radiance 2100 Rainbow laser scanning confocal microscope based on a Nikon E800 microscope.

Quantitative analyses were performed on three matched rostrocaudal sections separated by ~ 480 μm each [every ~12 sections; 40 μm section thickness (supplemental Fig. 1, available at www.jneurosci.org as supplemental material)]. Three adjacent fields defined by the 20× objective encompass the mediolateral extent of retrogradely labeled CSMN; the same systematically located fields were used for analysis in all mice. CSMN were counted only if their soma and apical dendrite were both visualized in the same thick 40 μm section. Representative sections and the locations of the three systematically located fields used for quantification of CSMN number and soma diameter in WT (P30, $n = 5$; P60, $n = 5$; P120, $n = 5$), hSOD1^{WT} (P30, $n = 5$; P60, $n = 5$; P120, $n = 5$), and

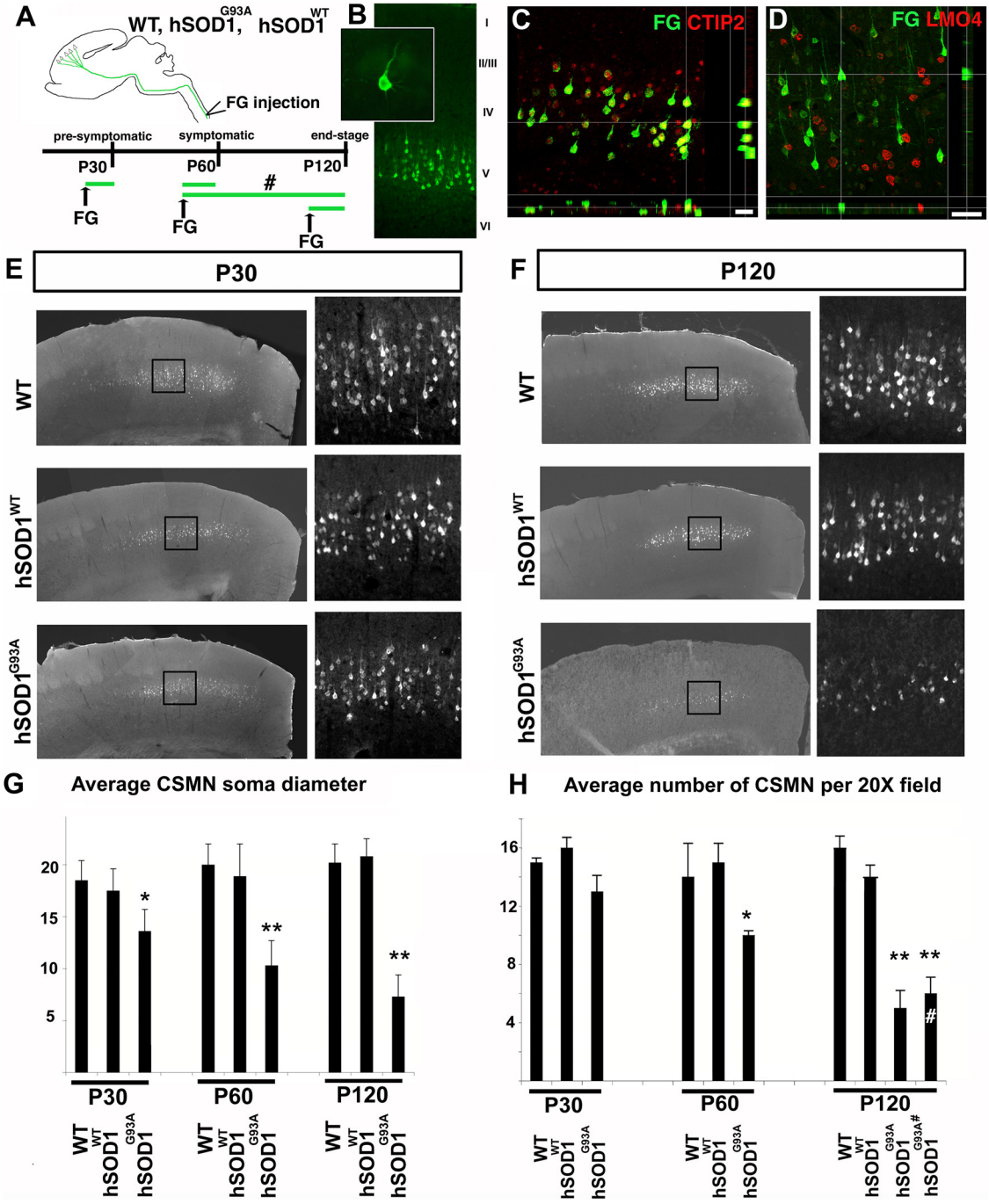

Figure 1. CSMN progressively degenerate in hSOD1^{G93A} mice. ***A***, Schematic diagram of experimental design. WT, hSOD1^{G93A}, and hSOD1^{WT} mice were retrogradely labeled by FluoroGold (FG) injections to be analyzed at P30 (presymptomatic), P60 (symptomatic), and P120 (end-stage). In a subset of experiments, CSMN were retrogradely labeled at P50 and analyzed at P120 (#). ***B***, Retrogradely labeled CSMN reside in layer V of the motor cortex and display distinct CSMN morphology (inset). ***C***, ***D***, Confocal analysis reveals colocalization of the CSMN/SCPN-specific (within neocortex) transcription factor CTIP2 (***C***) and exclusion of the CSMN-excluded transcription factor LMO4 (***D***) in retrogradely labeled CSMN. ***E***, ***F***, Comparable and representative coronal sections of the motor cortex from WT, hSOD1^{WT}, and hSOD1^{G93A} mice at P30 (***E***) and at P120 (***F***). The boxed areas are enlarged in the adjacent panels to show retrogradely labeled CSMN. ***G***, Bar graph representation of average CSMN soma diameter in WT, hSOD1^{WT}, and hSOD1^{G93A} mice at P30, P60, and P120. ***H***, Bar graph representation of the average number of CSMN per 20× field in WT, hSOD1^{WT}, and hSOD1^{G93A} mice at P30, P60, and P120. CSMN that were retrogradely labeled at P50 and analyzed at P120 are labeled with "#". Scale bars: ***C***, 40 μm; ***D***, 50 μm. Data are presented as mean ± SEM *$p < 0.05$; **$p < 0.0001$; ***G***, ***H***, Bonferroni test preceded by two-way ANOVA.

hSOD1^{G93A} (P30, $n = 5$; P60, $n = 5$; P120, $n = 8$) mice are shown in supplemental Figure 1 (available at www.jneurosci.org as supplemental material). For each mouse, a total of nine fields were counted (three fields in each of three sections), and numbers were averaged. All statistical analyses were performed with INSTAT software (version 3.0a; Graphpad); parametric and nonparametric multiple-comparison tests, such as Bonferroni and Tukey tests, were used where appropriate, with a minimum significance level set at $p < 0.05$.

Quantification of interneuron number was performed based on expression of PV and NPY. Three comparable 40 μm coronal sections that span the motor cortex (supplemental Fig. 1, available at www.jneurosci.org as supplemental material) from WT (P120, $n = 2$) and hSOD1^{G93A} (P120, $n = 3$) mice were analyzed. To perform unbiased and inclusive quantitative analysis, the cortex was divided into three equal sectors, mediolaterally/radially defined by equal 30° arcs. All neurons with both full cell bodies and immunopositivity for PV and NPY were counted in

each sector. All counts were performed "blinded" to the genotype of the sample by two independent observers. Interobserver variability was extremely low, with <3% variation between independent measurements.

To investigate the corticospinal tracts of Thy1-YFP;hSOD1^{G93A} mice (P30, $n = 2$; P60, $n = 3$; P120, $n = 4$) and Thy1-YFP;hSOD1^{WT} mice (P30, $n = 3$; P60, $n = 3$; P120, $n = 3$), spinal cords were isolated intact, and the cervical and lumbar segments of the spinal cords were sectioned axially (50 μm section thickness), whereas the thoracic segment was sectioned sagittally (150 μm section thickness). All thoracic segments containing axons were mounted on slides, and images of all sections that contained corticospinal tract axons were digitally collapsed to obtain a two-dimensional image to indicate the whole extent of the corticospinal tract. Representative axial sections of cervical and lumbar spinal cord were also imaged.

Results

CSMN progressively degenerate in hSOD1^{G93A} mice

We used a combination of anatomical and molecular approaches to identify, quantify, and assess potential vulnerability and progressive degeneration of CSMN. We retrogradely labeled CSMN by FG injection into the corticospinal tract within the dorsal funiculus of the C4–C6 region of the spinal cord (Fig. 1*A*). CSMN were retrogradely labeled at P20 for analysis at P30 (presymptomatic), at P50 for analysis at P60 (symptomatic), and at P100 for analysis at P120 (end-stage). In a subset of experiments designed to distinguish between genuine CSMN degeneration and potential appearance of reduced FG labeling due to defects in axonal transport, CSMN were retrogradely labeled at P50 and analyzed at P120 (Fig. 1*A*, "#"). P30, P60, and P120 times were chosen based on published and well established stages of disease progression with respect to both observed behavioral phenotypic changes and spinal motor neuron degeneration in hSOD1^{G93A} mice (Gurney et al., 1994; Hegedus et al., 2007). CSMN identity was established unequivocally by retrograde labeling from axon projections in the spinal cord, and verified based on (1) neuronal location in the primary motor cortex, (2) distinctive large CSMN morphology, and (3) expression of multiple recently identified positive and negative molecular markers that are either specifically expressed or excluded by CSMN (and related SCPN in some cases). Retrogradely labeled CSMN were confirmed to reside in layer V of the motor cortex and displayed distinct somatodendritic morphology of CSMN: they have a large pyramidal cell body and a long apical dendrite (Fig. 1*B*). Retrogradely labeled neurons expressed CTIP2 (Arlotta et al., 2005), a CSMN-specific (and cortico-brainstem; together, subcerebral-specific) transcription factor in layer V ($n = 150$, 100%) (Fig. 1*C*), and did not express LMO4, a transcription factor excluded from CSMN in layer V ($n = 120$, 0%) (Fig. 1*D*), confirming their CSMN identity. Although both CTIP2 and LMO4 expression levels are highest during development, and reduce with age, they remain specific and detectable (Fig. 1*C*,*D*) (see Materials and Methods). Homogeneity in the background of the WT, hSOD1^{WT}, and hSOD1^{G93A} mice, and the consistent copy number of transgenic gene expression (30 ± 2) in hSOD1^{WT} and hSOD1^{G93A} mice resulted in highly reproducible timing of disease onset and progression, enabling detailed and reproducible qualitative and quantitative analysis of CSMN degeneration at specific times during disease progression.

Qualitative analysis of retrogradely labeled CSMN in layer V of motor cortex in P30, P60, and P120 WT, hSOD1^{WT}, and hSOD1^{G93A} mice reveals dramatic CSMN vulnerability and marked degeneration in P120 hSOD1^{G93A} mice compared with WT and hSOD1^{WT} controls, present but more subtle at P30 and P60 (Fig. 1*E–H*). Quantitative analysis of CSMN soma diameter and neuron number at P30, P60, and P120 indicates progressive degeneration of CSMN only in hSOD1^{G93A} mice (Fig. 1*G*,*H*; supplemental Fig. 1, available at www.jneurosci.org as supplemental material). CSMN soma diameter in hSOD1^{G93A} mice significantly decreases, even during the "presymptomatic" stage (P30), and this decrease becomes even more striking with disease progression (Fig. 1*G*) (14 ± 2 μm at P30; 10 ± 2 μm at P60; 7 ± 2 μm at P120). In contrast, neither WT CSMN (19 ± 2 μm at P30; 20 ± 2 μm at P60; 20 ± 2 μm at P120) nor hSOD1^{WT} CSMN (18 ± 2 μm at P30; 19 ± 3 μm at P60; 21 ± 2 μm at P120) (supplemental Fig. 1, available at www.jneurosci.org as supplemental material) show any reduction in soma diameter.

Quantitative analysis of the number of CSMN in motor cortex indicates a progressive and dramatic degeneration of CSMN in hSOD1^{G93A} mice beginning by P30 (Fig. 1*H*) (13 ± 1 per 20× field at P30, $n = 5$ mice; 10 ± 1 at P60, $n = 6$ mice; 5 ± 2 at P120, $n = 8$ mice; 6 ± 1 at P120, injected at P50, $n = 3$ mice) (supplemental Fig. 1, available at www.jneurosci.org as supplemental material). In contrast, CSMN of neither WT (15 ± 1 at P30, $n = 5$ mice; 14 ± 2 at P60, $n = 5$ mice; 16 ± 2 at P120, $n = 6$ mice) nor hSOD1^{WT} mice (16 ± 1 at P30, $n = 4$ mice; 15 ± 2 at P60, $n = 5$ mice; 14 ± 1 at P120, $n = 5$ mice) demonstrate neuronal degeneration. At P120, hSOD1^{G93A} mice show identical numbers of retrogradely labeled CSMN, regardless of the time of retrograde labeling (5 ± 2 at P120, injected at P100, $n = 8$ mice; 6 ± 1 at P120, injected at P50, $n = 3$ mice), strongly indicating that CSMN undergo genuine somatic degeneration, and that the reduced number of retrogradely labeled CSMN is not due to confounding variables related to retrograde transport. In contrast, rubrospinal neurons, located in the red nucleus, and projecting to the cervical spinal cord (and thus also retrogradely labeled from the cervical spinal cord FG injections) are normal in number and morphology in hSOD1^{G93A} mice (as well as in hSOD1^{WT} and WT mice) at all ages including P120, reinforcing that degeneration is specific to CSMN in motor cortex in hSOD1^{G93A} mice (supplemental Fig. 2, available at www.jneurosci.org as supplemental material).

CSMN degeneration occurs via apoptosis

Investigation of CSMN death at all three stages of disease progression, using Nissl staining, analysis for nuclear pyknosis, and cleaved caspase-3 (CC-3) expression, reveals that CSMN death is apoptotic, and starts by P30 in hSOD1^{G93A} mice (Fig. 2). Nuclear pyknosis is an early sign of apoptotic cell death (de Rivero Vaccari et al., 2006), and CC-3 expression is detected in cells undergoing active apoptosis, although the time it takes CC-3-positive neurons to ultimately die is reported to take substantially longer *in vivo* than *in vitro* (Yang et al., 1998; Arai et al., 2005). Progressive apoptosis in hSOD1^{G93A} spinal motor neurons has been documented previously (Li et al., 2000; Przedborski, 2004; Wengenack et al., 2004), but CSMN were not investigated in detail. Here, all three analyses (Nissl, nuclear pyknosis, CC-3) reveal a wave of apoptotic CSMN death that starts by P30 in hSOD1^{G93A} mice. In striking contrast, WT and hSOD1^{WT} CSMN do not demonstrate neuronal death by any of these three modes of analysis at any stage investigated. At P30, apoptosis is visible by nuclear pyknosis (Fig. 2*A*) ($40 \pm 5\%$ of hSOD1^{G93A} CSMN, $n = 290$; $1 \pm 1\%$ of WT CSMN, $n = 271$; $3 \pm 1\%$ hSOD1^{WT} CSMN, $n = 264$) (Fig. 2*A*,*D*) and reduced soma size (Fig. 1*G*), and CC-3 expression is detected in some CSMN in hSOD1^{G93A} mice ($2 \pm 1\%$, $n = 148$), but not in WT or hSOD1^{WT}. To further investigate whether nuclear pyknosis, and thus neuronal degeneration, might begin even earlier than P30, we quantified nuclear pyknosis of CTIP2-

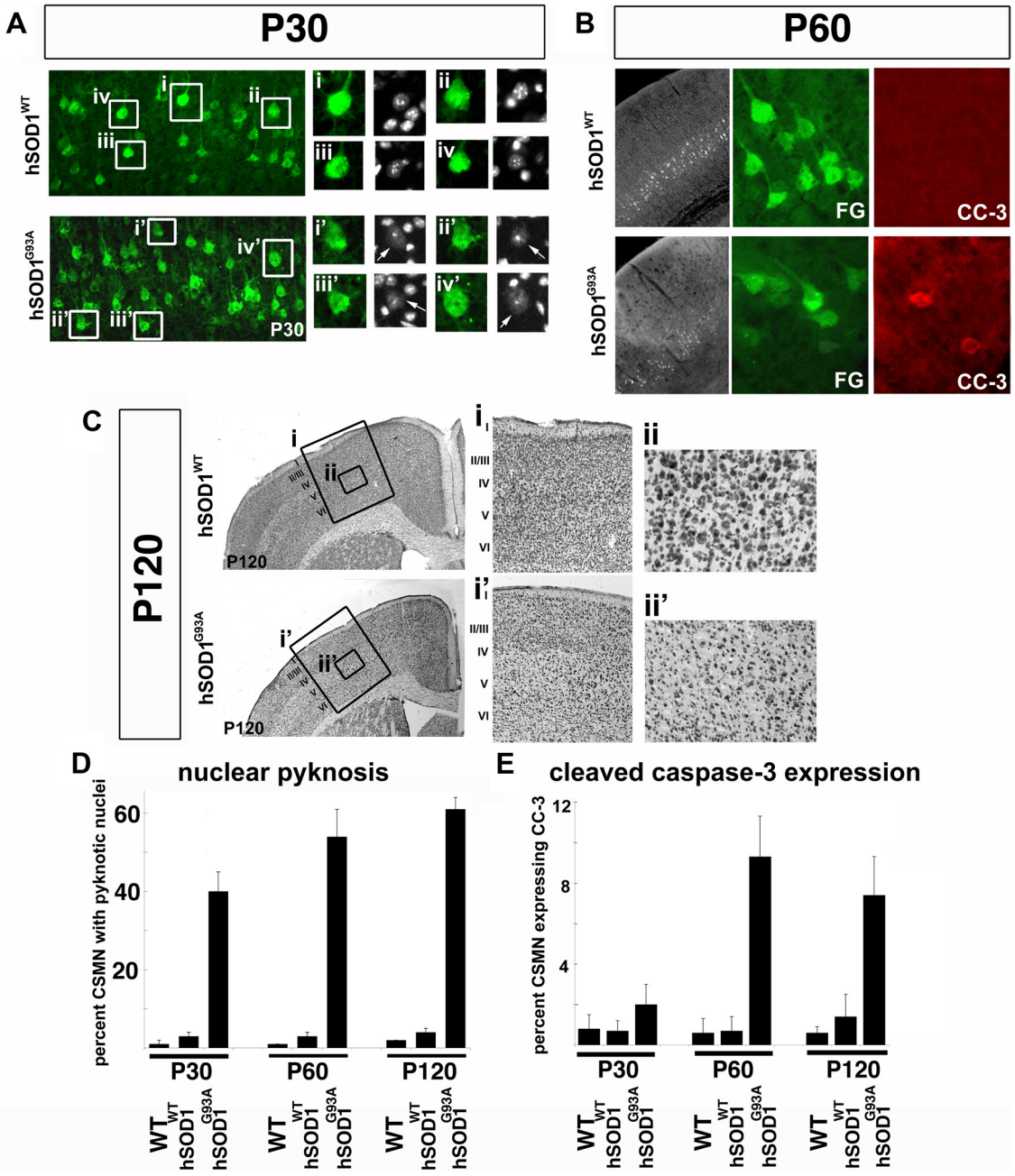

Figure 2. CSMN death occurs via apoptosis. ***A***, At P30, hSOD1^{WT} mice display healthy CSMN nuclei (***i–iv***), while apoptosis is visible by nuclear pyknosis in hSOD1^{G93A} CSMN (***i′–iv′***, arrows). The boxed areas (***i–iv***, ***i′–iv′***) in the low-magnification images are enlarged to the right. ***B***, At P60, CC-3 expression was increased in many hSOD1^{G93A} CSMN, but is not detected in hSOD1^{WT} CSMN. ***C***, At P120, Nissl stain analysis of motor cortex, and layer V in particular, reveals the normal complement of large pyramidal neurons in layer V of hSOD1^{WT} motor cortex (***i***, ***ii***) but a striking reduction in hSOD1^{G93A} motor cortex (***i′***, ***ii′***). The boxed areas (***i–ii′***) in the low-magnification images are enlarged to the right. ***D***, Bar graph representation of the percentage of CSMN with pyknotic nuclei at P30, P60, and P120 in WT, hSOD1^{WT}, and hSOD1^{G93A} mice. ***E***, Bar graph representation of the percentage of CSMN expressing CC-3, at P30, P60, and P120 in WT, hSOD1^{WT}, and hSOD1^{G93A} mice.

positive CSMN in layer V of motor cortex at P5, P10, and P15 compared with WT control CSMN at these same ages. These analyses reveal that 0% of WT CSMN display pyknotic nuclei at any of these early ages (P5, $n = 105$; P10, $n = 101$; P15, $n = 110$), whereas 2% of P5 hSOD1^{G93A} CSMN display pyknosis, $n = 114$; increasing to 4 ± 1% at P10, $n = 147$; and to 7 ± 1% at P15, $n = 112$. At P60, the percentages of CSMN with pyknotic nuclei (64 ± 3%, $n = 243$) or expressing CC-3 (9 ± 2%, $n = 140$) are substantially increased (Fig. 2*B*,*D*,*E*). At P120, CSMN degeneration in hSOD1^{G93A} mice is even more dramatic, with 7 ± 2% of CSMN expressing CC-3, 61 ± 3% with pyknotic nuclei, and near absence of large pyramidal neurons in layer V of motor cortex by Nissl staining (Fig. 2*C*). It is likely that CSMN detected at each age would include CSMN (1) already committed to die via apoptosis, (2) already dysfunctional and in the process of cell death, and (3) dead but not yet cleared from the tissue. These data suggest that many retrogradely labeled somata of CSMN detected in the cortex at P30, P60, and/or P120 are already less viable (likely already undergoing degeneration), but they are either not yet dead or not yet cleared from the tissue. Together, these results indicate by multiple independent criteria that progressive CSMN degeneration occurs in hSOD1^{G93A} mice, beginning early during the clas-

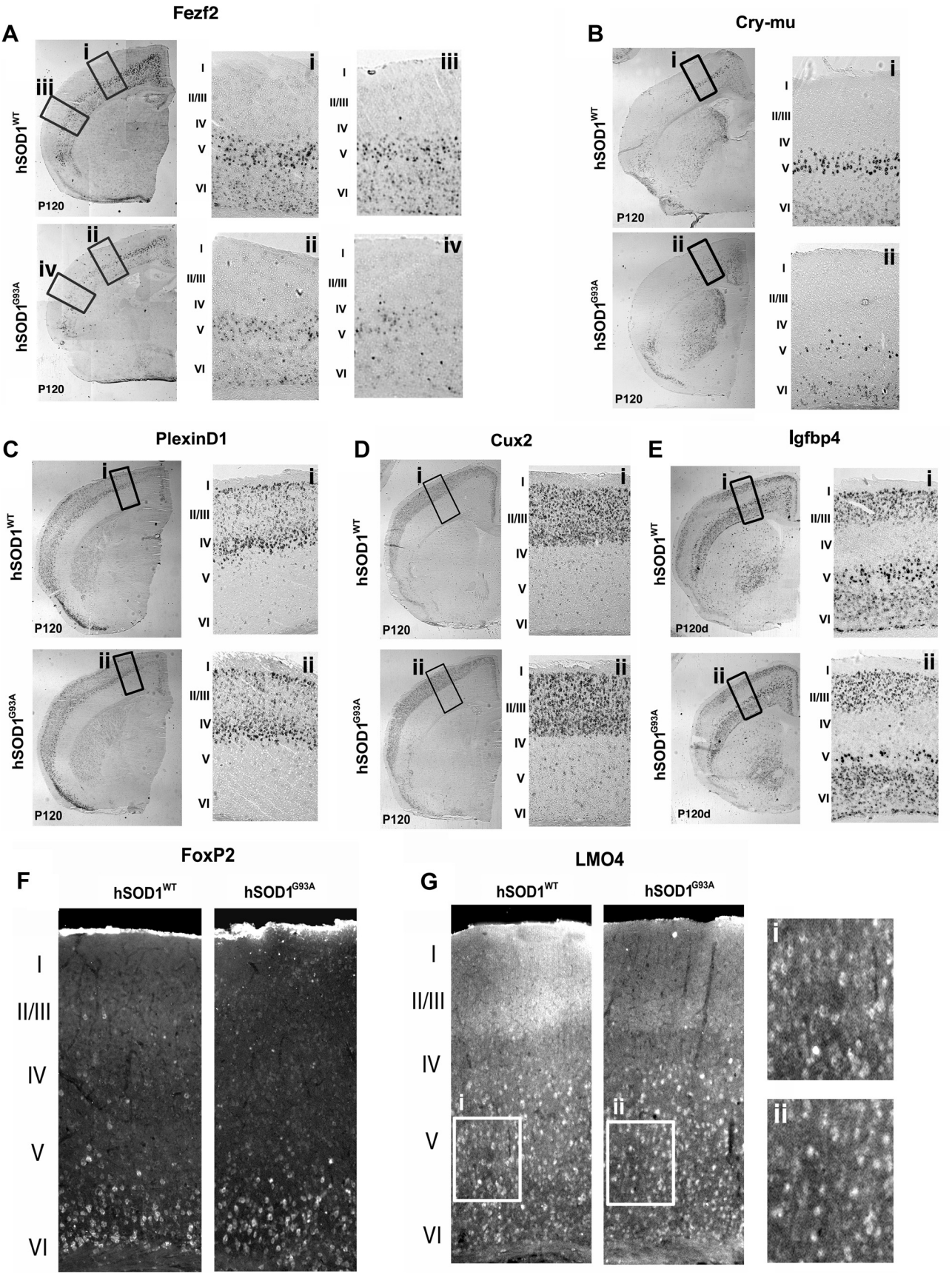

Figure 3. Degeneration is specific to CSMN and SCPN. ***A–E***, *In situ* hybridization analysis of *Fezf2* (***A***), *Cry-mu* (***B***), *PlexinD1* (***C***), *Cux2* (***D***), and *Igfbp4* (***E***) on coronal sections of hSOD1^{WT} and hSOD1^{G93A} cortex at P120. The boxed areas (***i–iv***) in the low-magnification images are enlarged to the right; roman numerals indicate the layers of motor cortex. *Fezf2* (***A***) is expressed at high levels in layer V of motor cortex (***i***) and nonmotor areas (***iii***) only in hSOD1^{WT} mice. *Fezf2* expression is dramatically reduced in the motor cortex (CSMN) (***ii***) and in the nonmotor areas of the cortex (SCPN) (*Figure legend continues.*)

sically presymptomatic stage, and mediated via apoptotic pathways.

Broader degeneration of developmentally related nonmotor subcerebral projection neurons occurs in hSOD1^{G93A} mice

To further investigate whether neocortical neuronal degeneration is specific to CSMN, or might involve other populations of cortical projection neurons and/or interneurons, we investigated the neuronal subtype identity and specificity of degeneration, using laminar and neuron type-specific molecular markers. We used a combination of immunocytochemical and *in situ* hybridization analyses in hSOD1^{G93A} and hSOD1^{WT} mice at P120. The results indicate that neuronal degeneration extends specifically to the developmentally related populations of motor and nonmotor, associative subcerebral projection neurons (SCPN), which include CSMN in the motor cortex. Neurons in other layers of the neocortex, and other neuron populations in layer V, are not affected.

Each molecular marker analyzed, both for CSMN/SCPN and for alternate neuron subtypes and lamina, confirms the specificity of CSMN/SCPN degeneration in the motor cortex of hSOD1^{G93A} mice. *Fezf2*, a transcription factor required for CSMN/SCPN specification and development, and expressed at high levels in CSMN/SCPN throughout life (Molyneaux et al., 2005; Molyneaux et al., 2007), has normal expression in hSOD1^{WT} mice at P120 (Fig. 3*A*). In contrast, *Fezf2* expression in motor cortex of hSOD1^{G93A} mice indicates dramatic loss of CSMN at P120 (Fig. 3*Ai*,*ii*). Interestingly, analysis of *Fezf2* expression in nonmotor areas of neocortex indicate additional involvement, but less striking loss, of the broader population of SCPN (Fig. 3*Aiii*,*iv*), which contribute to nonmotor cognitive, association, and integrative sensory systems in the cortex. *Cry-mu*, which is expressed at high levels by CSMN during development, and at very low levels by a subset of corticofugal neurons located in layer VI (Molyneaux et al., 2005; Molyneaux et al., 2007), displays normal expression in hSOD1^{WT} mice at P120 (Fig. 3*Bi*). In striking contrast, *cry-mu* expression confirms dramatic loss of CSMN in motor cortex in hSOD1^{G93A} mice (Fig. 3*Bii*). With regard to non-CSMN/SCPN populations, *PlexinD1* (Fig. 3*C*) and *Cux2* (Fig. 3*D*), both expressed in neuron populations in superficial layers of the neocortex during development through adulthood (Molyneaux et al., 2007), do not indicate any difference in superficial layer neuron populations in hSOD1^{G93A} versus hSOD1^{WT} mice. To further differentiate true CSMN/SCPN neuronal loss from simple gene dysregulation, *Igfbp4*, expressed at high levels by CSMN during development, and at lower levels in layer II/III and layer VI neurons in the cortex (Molyneaux et al., 2007), displays normal expression in all populations in hSOD1^{WT} mice at P120 (Fig. 3*E*). In contrast, in hSOD1^{G93A} mice, *Igfbp4* expression is sharply reduced in layer V (confirming CSMN/SCPN loss), while its expression is not affected in other neuron populations located in neocortical layers II/III and VI (Fig. 3*E*), further reinforcing the specificity of CSMN/SCPN degeneration in layer V of motor cortex. To even further consider whether neuronal degeneration is specific to CSMN/SCPN among the broader corticofugal populations (including, e.g., corticothalamic neurons), analysis of deepest layer VI of cortex for FoxP2 expression does not indicate any difference between hSOD1^{G93A} and hSOD1^{WT} mice (Fig. 3*F*). Similarly, LMO4, a transcription factor expressed by callosal projection neurons (inter-hemispheric, non-CSMN), interneurons, and other populations in layer V, but excluded from CSMN in layer V of the cortex (Arlotta et al., 2005; Molyneaux et al., 2005), is unchanged between hSOD1^{G93A} and hSOD1^{WT} mice (Fig. 3*Gi*,*ii*). In addition, dual retrograde labeling of CPN and CSMN at P30 in hSOD1^{G93A} and WT mice with perfusion at P120 indicates 1) no loss of CPN in hSOD1^{G93A} mice, 2) striking CSMN/SCPN-specific loss in hSOD1^{G93A} mice (again, labeled early to exclude retrograde transport as a confounding variable), 3) specificity of CSMN degeneration in motor cortex of hSOD1^{G93A} mice (supplemental Fig. 3, available at www.jneurosci.org as supplemental material).

Interneurons are not similarly affected in hSOD1^{G93A} mice

To investigate whether vulnerability and degeneration is restricted to CSMN/SCPN in the cortex of hSOD1^{G93A} mice, or whether nonprojection neuron populations (interneurons) are affected, we examined a broad variety of interneurons based on the interneuron molecular markers parvalbumin and neuropeptide Y (NPY) in both hSOD1^{G93A} ($n = 3$) and WT ($n = 2$) mice during the end-stage of disease progression. The results indicate that cortical interneuron populations are not apparently affected in hSOD1^{G93A} mice (Fig. 4). The number of parvalbumin-expressing interneurons does not differ substantially or significantly between hSOD1^{G93A} and WT mice, in any of the three mediolateral regions (Fig. 4*A–C*). Further, cellular morphologies of parvalbumin-positive cortical interneurons appear unchanged between WT and hSOD1^{G93A} mice, without suggestion of neuronal degeneration (Fig. 4*D*,*E*). Similar results were obtained for NPY-expressing interneurons (data not shown). A prior report suggested the possibility of interneuron degeneration in the cortex based on reduced cortical inhibition in ALS patients (Ziemann et al., 1997), but our analysis in hSOD1^{G93A} mice does not identify interneuron loss in these model mice. One recent study suggested increased cortical interneuron numbers in ALS mice, based on immunocytochemical analysis and applications of modeling (Minciacchi et al., 2009), but our results using broad mediolateral and rostrocaudal analysis do not identify such an increase. While it still remains possible that slight differences between the transgenic mice exist in localized areas, potentially secondary to degeneration of interneurons' CSMN/SCPN synaptic partners, we find no significant difference in interneurons more broadly between WT and hSOD1^{G93A} mouse neocortex.

Astrogliosis and microgliosis are present late during CSMN/SCPN degeneration

Activated astrocytes have been implicated in disease pathogenesis in ALS and have been detected both in ALS patient brains and spinal cords, and in spinal cords of hSOD1^{G93A} mice. To investigate whether astrogliosis (and, potentially, microglial activation) occurs in hSOD1^{G93A} mouse neocortex, and whether astrogliosis

←

(*Figure legend continued.*) (***iv***) in hSOD1^{G93A} mice. *Cry-mu* (***B***) is expressed at high levels in CSMN in hSOD1^{WT} mice (***i***), and *Cry-mu* expression is dramatically reduced in hSOD1^{G93A} mice (***ii***). *PlexinD1* (***C***) and *Cux2* (***D***), both expressed in neuron populations in superficial layers of the neocortex, show no difference between hSOD1^{WT} and hSOD1^{G93A} mice. *Igfbp4* (***E***) is expressed at high levels by CSMN and at lower levels in layer II/III and VI neurons in the cortex; hSOD1^{WT} mice display a normal complement of CSMN. In contrast, hSOD1^{G93A} mice have many fewer *Igfbp4*-expressing neurons in layer V, while other neuron populations are not affected, further confirming the specificity of CSMN degeneration. ***F***, FoxP2, expressed in the deepest layer VI of cortex, is unchanged between hSOD1^{WT} and hSOD1^{G93A} mice. ***G***, LMO4 expression, normally expressed by layer V callosal projection neurons, interneurons, and other populations, but excluded from CSMN in layer V, is unchanged between hSOD1^{WT} and hSOD1^{G93A} mice at P120 (***i***, ***ii***), reinforcing the specificity of CSMN degeneration in layer V of motor cortex in hSOD1^{G93A} mice.

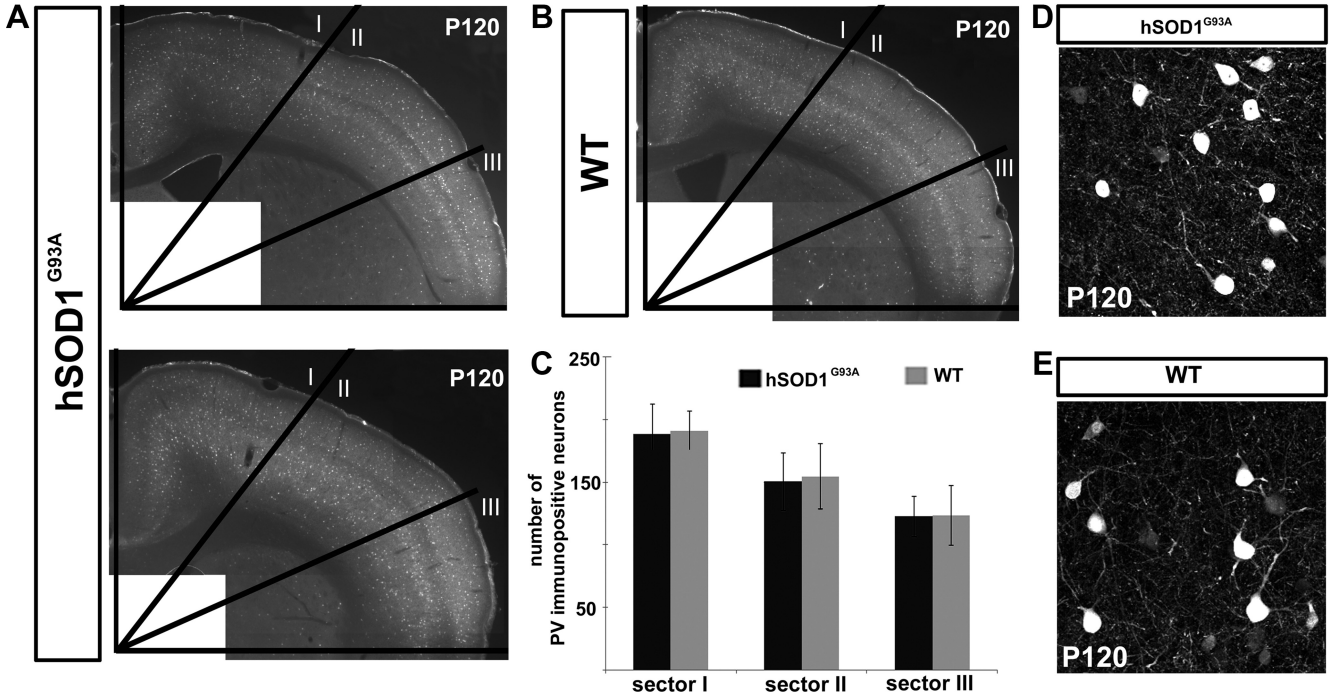

Figure 4. Cortical interneuron populations do not similarly degenerate in hSOD1^{G93A} mice. ***A–C***, PV-positive interneurons were quantified in hSOD1^{G93A} and WT mouse cortex at P120. The cortex was divided into three equal sectors and parvalbumin-positive neurons counted in each sector. ***A***, PV immunocytochemistry in coronal sections of two representative examples of hSOD1^{G93A} mouse cortex; one with the highest number of PV-positive interneurons (top) and one with the lowest number of PV-positive interneurons (bottom). ***B***, PV immunocytochemistry in a coronal cortical section of a representative WT mouse. ***C***, Bar graph displaying the total number of PV-positive neurons in each sector of the cortices from WT and hSOD1^{G93A} mice. ***D***, ***E***, Cellular morphologies of interneurons were unchanged between hSOD1^{G93A} (***D***) and WT mice (***E***), without suggestion of neuronal degeneration.

and/or microgliosis is present relatively early or late, we assessed the presence of activated astrocytes and/or microglia in hSOD1^{G93A} (P30, $n = 3$; P60, $n = 3$; P120, $n = 4$) and in hSOD1^{WT} (P30, $n = 2$; P60, $n = 2$; P120, $n = 3$) mice using GFAP and CD68 immunocytochemical analysis, respectively. We find that astrogliosis and microgliosis occur specifically in hSOD1^{G93A} mice (Fig. 5*A–I*, *M*) and not in hSOD1^{WT} mice (Fig. 5*J–L*). It occurs mainly at late stages of disease progression in hSOD1^{G93A} mice (Fig. 5*G–I*) and is not restricted to motor cortex (supplemental Fig. 4, available at www.jneurosci.org as supplemental material). These results suggest that CSMN/SCMN vulnerability and degeneration is initiated before astrogliosis and microgliosis in the neocortex of hSOD1^{G93A} mice.

The corticospinal tract degenerates in hSOD1^{G93A} mice

To investigate the time course of corticospinal tract (CST) degeneration in hSOD1^{G93A} mice that is the predicted accompaniment of the CSMN degeneration we identified in these mice, we applied genetic CST labeling using hSOD1^{G93A}, hSOD1^{WT}, and WT mice crossed with cortical-specific Thy1-YFP mice (Bareyre et al., 2005). In these mice, multiple populations of cortical pyramidal neurons express yellow fluorescent protein (YFP), while only CST axons are labeled in the spinal cord. As reflected by the "lateral sclerosis" component of its original pathologically descriptive name ("*sclerosis*" of the "*lateral*"—main—corticospinal tract in primates), CST degeneration is central to ALS, as an easily visible component of the degeneration of CSMN, whose axons form the CST. Mice with cortical specific Thy1-YFP neuron labeling were used to generate Thy1-YFP;hSOD1^{WT} and Thy1-YFP;hSOD1^{G93A} mice by serial breeding (see Materials and Methods) (Fig. 6*B*). Results from Thy1-YFP;hSOD1^{G93A} (P30, $n = 2$; P60, $n = 3$; P120, $n = 3$) (Fig. 6*A*, *B*) and Thy1-YFP; hSOD1^{WT} mice (P30, $n = 2$; P60, $n = 4$; P120, $n = 5$) (Fig. 6*B*) indicate that corticospinal tract degeneration is specific to Thy1-YFP;hSOD1^{G93A} mice. Degeneration is most dramatic between P60 and P120 (Fig. 6*D–F*). CST innervation of the lumbar spinal cord is essentially absent in Thy1-YFP;hSOD1^{G93A} mice by the late stages of disease progression (Fig. 6*Eiii*), and there is substantial loss of the cervical corticospinal tract (Fig. 6*Ei*). These results indicate that CSMN somal degeneration that occurs quite early is followed by profound corticospinal tract degeneration by late stages in hSOD1^{G93A} mice.

Discussion

Together, using a combination of anatomic, cellular, transgenic labeling, and newly available neuronal subtype-specific molecular analyses of both laminar and neuronal subtype identity, these results demonstrate that early and neuron type-specific CSMN/SCPN (both motor and nonmotor) neuronal degeneration is faithfully recapitulated in hSOD1^{G93A} transgenic ALS mice. Other neuron populations in other layers of the neocortex, other neuron populations within layer V, and interspersed cortical interneurons do not undergo such degeneration. Thus, hSOD1^{G93A} mice develop specific CSMN/SCPN degeneration that mirrors the cortical pathology found in human ALS, and nonmotor SCPN degeneration might explain some or much of the nonmotor cortical pathology identified in ALS. This neuron type-specific degeneration in hSOD1^{G93A} mice begins exceptionally early, in the presymptomatic stage, coincident with the earliest degeneration of spinal motor neurons (Gurney et al., 1994; Tu et al., 1996; Hall et al., 1998; Cleveland and Rothstein, 2001; Bruijn et al., 2004; Wengenack et al., 2004; Hegedus et al., 2007). These results are consistent with longstanding clinical evidence and more recent human magnetic resonance imaging

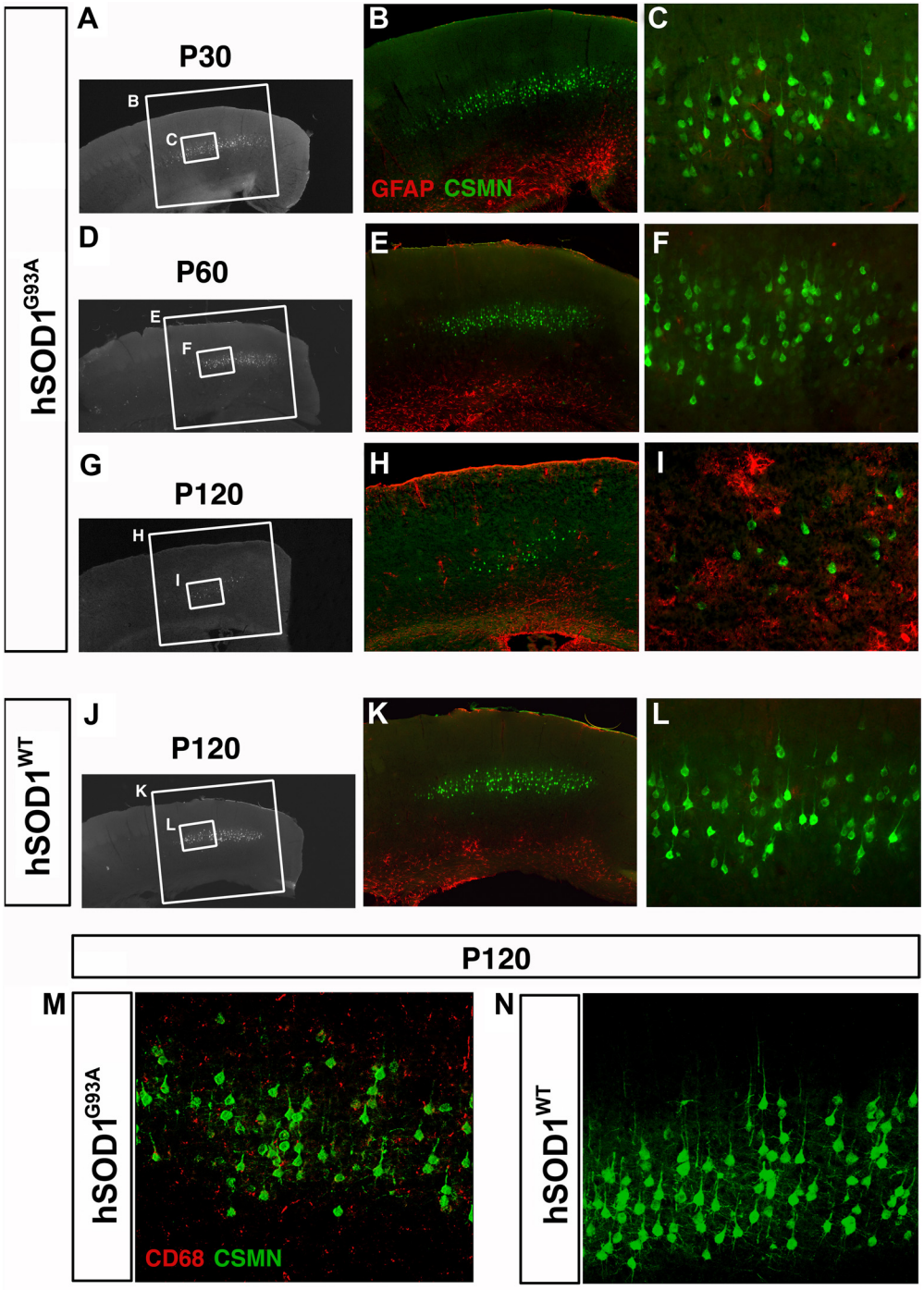

Figure 5. Astrogliosis and microgliosis is observed in hSOD1 ^{G93A} mice. ***A–I***, Astrogliosis in motor cortex of hSOD1 ^{G93A} mice at P30 (***A–C***), P60 (***D***, ***E***), and P120 (***G–I***). The boxed areas in the low-magnification images are enlarged to the right. Although progressive CSMN degeneration is observed in hSOD1 ^{G93A} mice at P30 to P60 (***B***, ***C***, ***E***, ***F***) and P120 (***B***, ***C***, ***E***, ***F***, ***H***, ***I***), activated astrocytes were first detected by GFAP expression later, here shown at P120 (***H***, ***I***). Astrogliosis was specific to hSOD1 ^{G93A} mice, and hSOD1 ^{WT} mice do not display activated astrocytes at P120 (***J–L***). Similarly, activated microglia were detected by CD68 expression only in hSOD1 ^{G93A} cortex (***M***) and not in hSOD1 ^{WT} cortex (***N***) at P120.

studies that clearly indicate that CSMN in motor cortex are affected at early stages of ALS (Brown, 2005; Graham et al., 2004; Stewart et al., 2006). The data reveal early events of CSMN degeneration by P30, with progressive CSMN degeneration occurring via apoptosis. Neocortical neuron degeneration is specific to CSMN/SCPN in the cerebral cortex of hSOD1 ^{G93A} mice. In contrast, other cortical neuron populations do not undergo such degeneration—other cortical projection neuron populations in other layers of the cortex, other projection neuron populations within cortical layer V, or interneurons. CSMN undergo true cellular degeneration, not simply defects in retrograde axonal transport, shown to be separable issues by multistage retrograde labeling experiments. CSMN-specific degeneration is accompanied by striking corticospinal tract degeneration later in disease progression, revealed by transgenic labeling of corticospinal tract axons in Thy1-YFP;hSOD1 ^{G93A} mice. These experiments and findings provide a foundation for detailed investigation of CSMN/SCPN

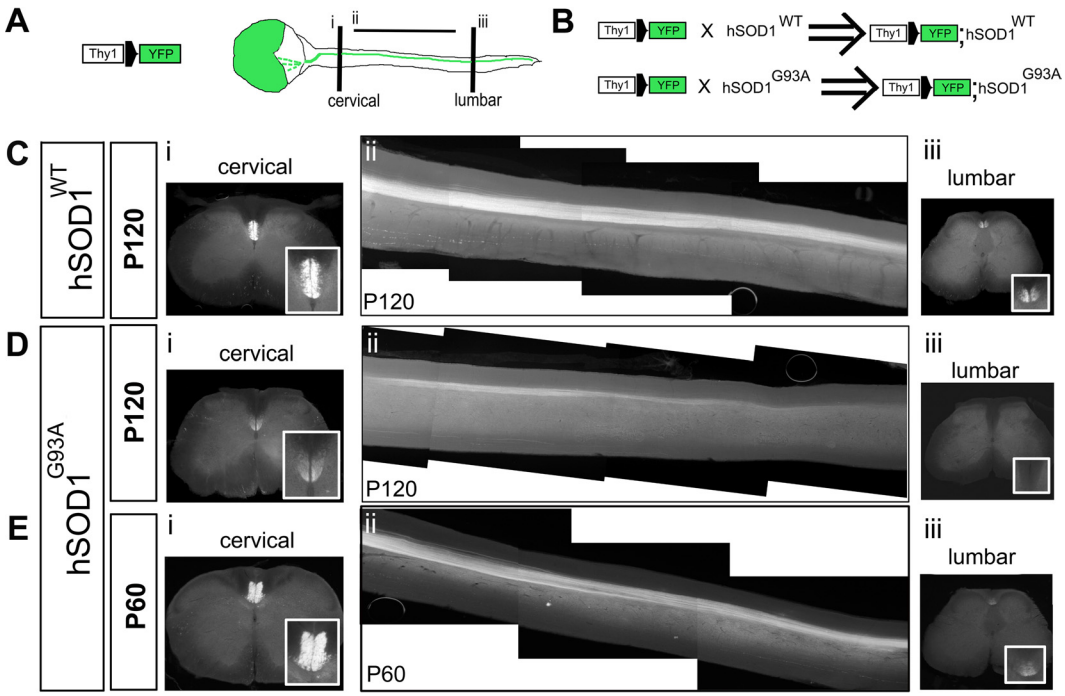

Figure 6. The corticospinal tract degenerates in Thy1-YFP;hSOD1^{G93A} mice. ***A***, Breeding of hSOD1 transgenic mice with Thy1-YFP transgenic mice was used to visualize the CST in hSOD1^{G93A} and hSOD1^{WT} mice. Schematic drawing of cerebral cortex and spinal cord of Thy1-YFP transgenic mice, in which the CST is visualized by YFP fluorescence in the spinal cord. Cervical and lumbar segments of the spinal cord were investigated by single 50-μm-thick axial sections (***i***, ***iii***). Sagittal sections were used for the thoracic cord; to identify the entire extent of the CST in the thoracic segment, all 150-μm-thick sagittal sections containing CST axons were digitally collapsed into a single two-dimensional image (***ii***). ***B***, Thy1-YFP;hSOD1^{G93A} and Thy1-YFP;hSOD1^{WT} mice (hemizygous for both the Thy1-YFP and the hSOD1^{G93A} genes) were generated by serial breeding Thy1-YFP mice and hSOD1^{G93A} or hSOD1^{WT} mice, respectively. Thy1-YFP;WT mice were used as controls. ***C–E***, Insets (***Ci***, ***Di***, ***Ei***, ***Ciii***, ***Diii***, ***Eiii***) show higher-magnification views of the dorsal funiculi, indicating CST axons at both the cervical (***i***) and lumbar (***iii***) segments of the spinal cord. ***C***, At P120, the CST did not show any sign of degeneration in Thy1-YFP;hSOD1^{WT} mice. The CST is normal in the cervical (***i***), thoracic (***ii***), and lumbar spinal cord (***iii***). ***D***, ***E***, In Thy1-YFP;hSOD1^{G93A} mice, CST degeneration is most dramatic between P60 and P120. There is substantial loss of cervical (***Di***) and thoracic (***Dii***) CST axons by P120, and innervation of the lumbar spinal cord is drastically reduced to absent in Thy1-YFP;hSOD1^{G93A} mice at P120 (***Diii***).

biology in ALS, and of potentially shared biology between CSMN and SMN upper and lower motor neurons, respectively.

It is quite notable that CSMN degeneration is accompanied by degeneration of the related broader category of SCPN. Types of SCPN other than CSMN are molecularly and developmentally closely related to CSMN, and their coincident degeneration might be in part responsible for the broader cortical pathology in cognitive, association, and even sensory systems in many ALS cases. This further links the findings in hSOD1^{G93A} mice to this emergingly important biology in humans with ALS. To further our understanding of CSMN/SCPN degeneration in human ALS, neuron type-specific analysis coupled with cellular and genetic labeling now enables deeper investigation regarding the cortical component of pathology in hSOD1^{G93A} mice. Such investigation can now build on both basic anatomical analysis of the cortex/corticospinal tract, and on new molecular knowledge about subtype-specific differentiation and markers (Arlotta et al., 2005; Molyneaux et al., 2005, 2007, 2009; Tomassy et al., 2010). Using a combination of anatomical, cellular, transgenic labeling, and newly available neuronal subtype-specific molecular analyses to identify, quantify, and assess progressive and neuron type-specific degeneration of CSMN and related SCPN in hSOD1^{G93A} transgenic ALS mice, these experiments closely link the mouse and human corticospinal and broader cortical biology of ALS. These analyses can now be extended by other investigators to other mammalian models of ALS to more deeply and rigorously elucidate the extent and mechanisms of cortical pathology. Such investigations will likely also elucidate mechanisms of CSMN/SCPN degeneration in other upper motor neuron neurodegenerative diseases, such as hereditary spastic paraplegia and primary lateral sclerosis.

CSMN and SMN degenerate independently, but their degeneration is potentially mechanistically related. CSMN and SMN are located at distant locations in the CNS, have very different developmental histories, and are positioned in distinct but potentially related microenvironments (with related glutamatergic synapses, transmission, and functions of surrounding astroglia, and potentially some shared channel properties). However, their progressive and specific degeneration indicates the relevance and importance of potentially common biology between these upper and lower motor neurons in ALS.

Sufficient information is developing to begin to elucidate common and/or unique biology between CSMN and SMN during development, and in ALS and related neurodegenerative diseases. There has been deep and important work on the differentiation, development, and maturation of spinal motor neurons (Tanabe and Jessell, 1996; Ericson et al., 1997; Arber et al., 1999; Briscoe et al., 1999; Pierani et al., 2001; Wichterle et al., 2002; William et al., 2003; Dasen et al., 2003, 2005; Kania and Jessell, 2003; Lanuza et al., 2004; Fox et al., 2007; Azim et al., 2009a,b; Molyneaux et al., 2009). In addition, cellular and molecular controls over differentiation, development, and maturation of CSMN/SCPN and other populations of neocortical projection neurons are beginning to emerge (Arlotta et al., 2005; B. Chen et al., 2005; J. G. Chen et al., 2005; Molyneaux et al., 2005, 2007, 2009; Ozdinler and Macklis, 2006; Joshi et al., 2008; Lai et al., 2008; Azim et al., 2009a,b; Tomassy et al., 2010). Moreover,

there have been multiple recent studies investigating early defects in corticospinal motor neuron circuitry in the cerebral cortex of ALS patients and the progressive cortical pathology with respect to spinal motor neuron degeneration (Vucic et al., 2008; Sivák et al., 2010; van der Graaff et al., 2010; Mohammadi et al., 2011). Emerging evidence also indicates the relevance of SOD1 pathology in at least some sporadic ALS cases and extends the importance of understanding SOD1-mediated pathology well beyond familial ALS (Bosco et al., 2010). These studies, together with increasing understanding regarding the biology of both upper and lower motor neurons, might contribute toward development of future diagnostic and therapeutic approaches.

Understanding cellular and molecular mechanisms of cell type-specific degeneration in neurodegenerative diseases is of major and important interest toward both prevention and therapy. Together, our investigations establish and clarify the central, early, specific, and independent involvement of CSMN/SCPN in hSOD1^{G93A} mice, and develop neuron type-specific approaches for analysis of the upper motor neuron component of neurodegeneration and its potential prevention or therapy in hSOD1^{G93A} mice and other rodent models of ALS.

References

Arai M, Sasaki A, Saito N, Nakazato Y (2005) Immunohistochemical analysis of cleaved caspase-3 detects high level of apoptosis frequently in diffuse large B-cell lymphomas of the central nervous system. Pathol Int 55:122–129.

Arber S, Han B, Mendelsohn M, Smith M, Jessell TM, Sockanathan S (1999) Requirement for the homeobox gene Hb9 in the consolidation of motor neuron identity. Neuron 23:659–674.

Arlotta P, Molyneaux BJ, Chen J, Inoue J, Kominami R, Macklis JD (2005) Neuronal subtype-specific genes that control corticospinal motor neuron development in vivo. Neuron 45:207–221.

Azim E, Jabaudon D, Fame RM, Macklis JD (2009a) SOX6 controls dorsal progenitor identity and interneuron diversity during neocortical development. Nat Neurosci 12:1238–1247.

Azim E, Shnider SJ, Cederquist GY, Sohur US, Macklis JD (2009b) Lmo4 and Clim1 progressively delineate cortical projection neuron subtypes during development. Cereb Cortex 19 [Suppl 1]:i62–69.

Bareyre FM, Kerschensteiner M, Misgeld T, Sanes JR (2005) Transgenic labeling of the corticospinal tract for monitoring axonal responses to spinal cord injury. Nat Med 11:1355–1360.

Beckman JS, Estévez AG, Crow JP, Barbeito L (2001) Superoxide dismutase and the death of motoneurons in ALS. Trends Neurosci 24:S15–20.

Bendotti C, Carrì MT (2004) Lessons from models of SOD1-linked familial ALS. Trends Mol Med 10:393–400.

Boillée S, Cleveland DW (2004) Gene therapy for ALS delivers. Trends Neurosci 27:235–238.

Bosco DA, Morfini G, Karabacak NM, Song Y, Gros-Louis F, Pasinelli P, Goolsby H, Fontaine BA, Lemay N, McKenna-Yasek D, Frosch MP, Agar JN, Julien JP, Brady ST, Brown RH Jr (2010) Wild-type and mutant SOD1 share an aberrant conformation and a common pathogenic pathway in ALS. Nat Neurosci 13:1396–1403.

Briscoe J, Sussel L, Serup P, Hartigan-O'Connor D, Jessell TM, Rubenstein JL, Ericson J (1999) Homeobox gene Nkx2.2 and specification of neuronal identity by graded Sonic hedgehog signalling. Nature 398:622–627.

Brown RH Jr, Robberecht W (2001) Amyotrophic lateral sclerosis: pathogenesis. Semin Neurol 21:131–139.

Brown RH Jr (2005) Amyotrophic lateral sclerosis. In: Harrison's textbook of internal medicine, Ed 16 (S.L. Hauser, D.L. Kasper, E. Braunwald, A.S. Fauci, L. Jameson, K.J. Isselbacher, eds).

Bruijn LI, Miller TM, Cleveland DW (2004) Unraveling the mechanisms involved in motor neuron degeneration in ALS. Annu Rev Neurosci 27:723–749.

Chen B, Schaevitz LR, McConnell SK (2005) Fezl regulates the differentiation and axon targeting of layer 5 subcortical projection neurons in cerebral cortex. Proc Natl Acad Sci U S A 102:17184–17189.

Chen JG, Rasin MR, Kwan KY, Sestan N (2005) Zfp312 is required for subcortical axonal projections and dendritic morphology of deep-layer pyramidal neurons of the cerebral cortex. Proc Natl Acad Sci U S A 102:17792–17797.

Chiu AY, Zhai P, Dal Canto MC, Peters TM, Kwon YW, Prattis SM, Gurney ME (1995) Age-dependent penetrance of disease in a transgenic mouse model of familial amyotrophic lateral sclerosis. Mol Cell Neurosci 6:349–362.

Cleveland DW, Rothstein JD (2001) From Charcot to Lou Gehrig: deciphering selective motor neuron death in ALS. Nat Rev Neurosci 2:806–819.

Dasen JS, Liu JP, Jessell TM (2003) Motor neuron columnar fate imposed by sequential phases of Hox-c activity. Nature 425:926–933.

Dasen JS, Tice BC, Brenner-Morton S, Jessell TM (2005) A Hox regulatory network establishes motor neuron pool identity and target-muscle connectivity. Cell 123:477–491.

de Rivero Vaccari JC, Casey GP, Aleem S, Park WM, Corriveau RA (2006) NMDA receptors promote survival in somatosensory relay nuclei by inhibiting Bax-dependent developmental cell death. Proc Natl Acad Sci U S A 103:16971–16976.

Ericson J, Rashbass P, Schedl A, Brenner-Morton S, Kawakami A, van Heyningen V, Jessell TM, Briscoe J (1997) Pax6 controls progenitor cell identity and neuronal fate in response to graded Shh signaling. Cell 90:169–180.

Fink JK (2002) Hereditary spastic paraplegia: the pace quickens. Ann Neurol 51:669–672.

Fink JK (2006) Hereditary spastic paraplegia. Curr Neurol Neurosci Rep 6:65–76.

Fox MA, Sanes JR, Borza DB, Eswarakumar VP, Fassler R, Hudson BG, John SW, Ninomiya Y, Pedchenko V, Pfaff SL, Rheault MN, Sado Y, Segal Y, Werle MJ, Umemori H (2007) Distinct target-derived signals organize formation, maturation, and maintenance of motor nerve terminals. Cell 129:179–193.

Gavrilina TO, McGovern VL, Workman E, Crawford TO, Gogliotti RG, Didonato CJ, Monani UR, Morris GE, and Burghes HM (2008) Neuronal SMN expression corrects spinal muscular atrophy in severe SMA mice while muscle specific SMN expression has no phenotypic effect. Hum Mol Genet 17:1063–1075.

Graham JM, Papadakis N, Evans J, Widjaja E, Romanowski CA, Paley MN, Wallis LI, Wilkinson ID, Shaw PJ, Griffiths PD (2004) Diffusion tensor imaging for the assessment of upper motor neuron integrity in ALS. Neurology 63:2111–2119.

Gurney ME (1997) The use of transgenic mouse models of amyotrophic lateral sclerosis in preclinical drug studies. J Neurol Sci 152 [Suppl 1]:S67–S73.

Gurney ME (2000) What transgenic mice tell us about neurodegenerative disease. Bioessays 22:297–304.

Gurney ME, Pu H, Chiu AY, Dal Canto MC, Polchow CY, Alexander DD, Caliendo J, Hentati A, Kwon YW, Deng HX, Cheng W, Zhai P, Sufit RL, Siddique T (1994) Motor neuron degeneration in mice that express a human Cu,Zn superoxide dismutase mutation. Science 264:1772–1775.

Hall ED, Oostveen JA, Gurney ME (1998) Relationship of microglial and astrocytic activation to disease onset and progression in a transgenic model of familial ALS. Glia 23:249–256.

Hegedus J, Putman CT, Gordon T (2007) Time course of preferential motor unit loss in the SOD1 G93A mouse model of amyotrophic lateral sclerosis. Neurobiol Dis 28:154–164.

Joshi PS, Molyneaux BJ, Feng L, Xie X, Macklis JD, Gan L (2008) Bhlhb5 regulates the postmitotic acquisition of area identities in layers II-V of the developing neocortex. Neuron 60:258–272.

Kania A, Jessell TM (2003) Topographic motor projections in the limb imposed by LIM homeodomain protein regulation of ephrin-A:EphA interactions. Neuron 38:581–596.

Kunst CB, Mezey E, Brownstein MJ, Patterson D (1997) Mutations in SOD1 associated with amyotrophic lateral sclerosis cause novel protein interactions. Nat Genet 15:91–94.

Lai T, Jabaudon D, Molyneaux BJ, Azim E, Arlotta P, Menezes JR, Macklis JD (2008) SOX5 controls the sequential generation of distinct corticofugal neuron subtypes. Neuron 57:232–247.

Lanuza GM, Gosgnach S, Pierani A, Jessell TM, Goulding M (2004) Genetic identification of spinal interneurons that coordinate left-right locomotor activity necessary for walking movements. Neuron 42:375–386.

Lefebvre S, Bürglen L, Frézal J, Munnich A, Melki J (1998) The role of the

SMN gene in proximal spinal muscular atrophy. Hum Mol Genet 7:1531–1536.

Li M, Ona VO, Guégan C, Chen M, Jackson-Lewis V, Andrews LJ, Olszewski AJ, Stieg PE, Lee JP, Przedborski S, Friedlander RM (2000) Functional role of caspase-1 and caspase-3 in an ALS transgenic mouse model. Science 288:335–339.

Lobsiger CS, Garcia ML, Ward CM, Cleveland DW (2005) Altered axonal architecture by removal of the heavily phosphorylated neurofilament tail domains strongly slows superoxide dismutase 1 mutant-mediated ALS. Proc Natl Acad Sci U S A 102:10351–10356.

Lomen-Hoerth C, Murphy J, Langmore S, Kramer JH, Olney RK, Miller B (2003) Are amyotrophic lateral sclerosis patients cognitively normal? Neurology 60:1094–1097.

Minciacchi D, Kassa RM, Del Tongo C, Mariotti R, Bentivoglio M (2009) Voronoi-based spatial analysis reveals selective interneuron changes in the cortex of FALS mice. Exp Neurol 215:77–86.

Mohammadi B, Kollewe K, Samii A, Dengler R, Munte TF (2011) Functional neuroimaging at different disease stages reveals distinct phases of neuroplastic changes in amyotrophic lateral sclerosis. Hum Brain Mapp. Advance online publication. Retrieved October 15, 2010. doi: 10.1002/hbm.21064.

Molyneaux BJ, Arlotta P, Hirata T, Hibi M, Macklis JD (2005) Fezl is required for the birth and specification of corticospinal motor neurons. Neuron 47:817–831.

Molyneaux BJ, Arlotta P, Menezes JR, Macklis JD (2007) Neuronal subtype specification in the cerebral cortex. Nat Rev Neurosci 8:427–437.

Molyneaux BJ, Arlotta P, Fame RM, MacDonald JL, MacQuarrie KL, Macklis JD (2009) Novel subtype-specific genes identify distinct subpopulations of callosal projection neurons. J Neurosci 29:12343–12354.

Niessen HG, Angenstein F, Sander K, Kunz WS, Teuchert M, Ludolph AC, Heinze HJ, Scheich H, Vielhaber S (2006) In vivo quantification of spinal and bulbar motor neuron degeneration in the G93A-SOD1 transgenic mouse model of ALS by T2 relaxation time and apparent diffusion coefficient. Exp Neurol 201:293–300.

Ozdinler PH, Macklis JD (2006) IGF-I specifically enhances axon outgrowth of corticospinal motor neurons. Nat Neurosci 9:1371–1381.

Pasinelli P, Brown RH (2006) Molecular biology of amyotrophic lateral sclerosis: insights from genetics. Nat Rev Neurosci 7:710–723.

Pierani A, Moran-Rivard L, Sunshine MJ, Littman DR, Goulding M, Jessell TM (2001) Control of interneuron fate in the developing spinal cord by the progenitor homeodomain protein Dbx1. Neuron 29:367–384.

Przedborski S (2004) Programmed cell death in amyotrophic lateral sclerosis: a mechanism of pathogenic and therapeutic importance. Neurologist 10:1–7.

Rainier S, Chai JH, Tokarz D, Nicholls RD, Fink JK (2003) NIPA1 gene mutations cause autosomal dominant hereditary spastic paraplegia (SPG6). Am J Hum Genet 73:967–971.

Ralph GS, Radcliffe PA, Day DM, Carthy JM, Leroux MA, Lee DC, Wong LF, Bilsland LG, Greensmith L, Kingsman SM, Mitrophanous KA, Mazarakis ND, Azzouz M (2005) Silencing mutant SOD1 using RNAi protects against neurodegeneration and extends survival in an ALS model. Nat Med 11:429–433.

Rösler KM, Truffert A, Hess CW, Magistris MR (2000) Quantification of upper motor neuron loss in amyotrophic lateral sclerosis. Clin Neurophysiol 111:2208–2218.

Sivák S, Bittšanský M, Kurča E, Turčanová-Koprušáková M, Grofik M, Nosál′ V, Poláček, Dobrota D (2010) Proton magnetic resonance spectroscopy in patients with early stages of amyotrophic lateral sclerosis. Neuroradiology 52:1079–1085.

Stewart HG, Andersen PM, Eisen A, Weber M (2006) Corticomotoneuronal dysfunction in ALS patients with different SOD1 mutations. Clin Neurophysiol 117:1850–1861.

Strong MJ (2008) The syndromes of frontotemporal dysfunction in amyotrophic lateral sclerosis. Amyotroph Lateral Scler 9:323–338.

Tanabe Y, Jessell TM (1996) Diversity and pattern in the developing spinal cord. Science 274:1115–1123.

Tomassy GS, De Leonibus E, Jabaudon D, Lodato S, Alfano C, Mele A, Macklis JD, Studer M (2010) Area-specific temporal control of corticospinal motor neuron differentiation by COUP-TFI. Proc Natl Acad Sci U S A 107:3576–3581.

Tu PH, Raju P, Robinson KA, Gurney ME, Trojanowski JQ, Lee VM (1996) Transgenic mice carrying a human mutant superoxide dismutase transgene develop neuronal cytoskeletal pathology resembling human amyotrophic lateral sclerosis lesions. Proc Natl Acad Sci U S A 93:3155–3160.

Turner BJ, Talbot K (2008) Transgenics, toxicity and therapeutics in rodent models of mutant SOD1-mediated familial ALS. Prog Neurobiol 85:94–134.

van der Graaff MM, Lavini C, Akkerman EM, Majoie Ch B, Nederveen AJ, Zwinderman AH, Brugman F, van den Berg LH, de Jong JM, de Visser M (2010) MR Spectroscopy Findings in Early Stages of Motor Neuron Disease. AJNR Am J Neuroradiol 31:1799–1806.

Vucic S, Nicholson GA, Kiernan MC (2008) Cortical hyperexcitability may precede the onset of familial amyotrophic lateral sclerosis. Brain 131:1540–1550.

Wengenack TM, Holasek SS, Montano CM, Gregor D, Curran GL, Poduslo JF (2004) Activation of programmed cell death markers in ventral horn motor neurons during early presymptomatic stages of amyotrophic lateral sclerosis in a transgenic mouse model. Brain Res 1027:73–86.

Wichterle H, Lieberam I, Porter JA, Jessell TM (2002) Directed differentiation of embryonic stem cells into motor neurons. Cell 110:385–397.

William CM, Tanabe Y, Jessell TM (2003) Regulation of motor neuron subtype identity by repressor activity of Mnx class homeodomain proteins. Development 130:1523–1536.

Wong PC, Cai H, Borchelt DR, Price DL (2002) Genetically engineered mouse models of neurodegenerative diseases. Nat Neurosci 5:633–639.

Yamanaka K, Miller TM, McAlonis-Downes M, Chun SJ, Cleveland DW (2006) Progressive spinal axonal degeneration and slowness in ALS2-deficient mice. Ann Neurol 60:95–104.

Yang F, Sun X, Beech W, Teter B, Wu S, Sigel J, Vinters HV, Frautschy SA, Cole GM (1998) Antibody to caspase-cleaved actin detects apoptosis in differentiated neuroblastoma and plaque-associated neurons and microglia in Alzheimer's disease. Am J Pathol 152:379–389.

Zanette G, Tamburin S, Manganotti P, Refatti N, Forgione A, Rizzuto N (2002) Changes in motor cortex inhibition over time in patients with amyotrophic lateral sclerosis. J Neurol 249:1723–1728.

Zang DW, Cheema SS (2002) Degeneration of corticospinal and bulbospinal systems in the superoxide dismutase 1(G93A G1H) transgenic mouse model of familial amyotrophic lateral sclerosis. Neurosci Lett 332:99–102.

Ziemann U, Winter M, Reimers CD, Reimers K, Tergau F, Paulus W (1997) Impaired motor cortex inhibition in patients with amyotrophic lateral sclerosis. Evidence from paired transcranial magnetic stimulation. Neurology 49:1292–1298.